Journal of Computational and Applied Mechanics, Vol. 6., No. 2., (2005), pp. 311–319

NUMERICAL SIMULATION OF THE DYNAMICS OF A NONLOCAL, INHOMOGENEOUS, INFINITE BAR

Olaf Weckner
Massachusetts Institute of Technology
Department of Mechanical Engineering
Cambridge, MA 02139, USA
olaf@weckner.de

Etienne Emmrich
Technische Universität Berlin
Institut für Mathematik
Straße des 17. Juni 135, 10623 Berlin, Germany
emmrich@math.tu-berlin.de

[Received: January 31, 2005]

Abstract. In this paper, we develop an efficient numerical method based on Gauß-Hermite quadrature to calculate the one-dimensional dynamic response of a nonlocal, peridynamic bar composed of (inhomogeneous) linear material. The principal *physical* characteristic of the peridynamic theory is the presence of long-range forces leading to nonlinear dispersion relations while the principal *mathematical* characteristic is the presence of a stationary Barbashin operator in the integro-differential equation of motion. We calculate two examples corresponding to continuous and discontinuous, Riemann-like initial conditions. As the analytical solutions for these examples are known, they serve as validation problems for the proposed numerical scheme.

Mathematical Subject Classification: 74H15, 65R20, 45K05
Keywords: integro-differential equation, quadrature, Barbashin operator, long-range forces, nonlocal, peridynamic

1. Introduction

In the classical *local* theory of elasticity, the equation of motion is a partial differential equation (PDE). However, if *nonlocal* effects have to be considered, it can[1] become an integro-differential equation (IDE), see Silling [2], Kunin [3] and Rogula [4]. For an infinite, homogeneous, linear microelastic bar, this 'peridynamic' equation of motion

[1]There are numerous approaches to model nonlocality which do not necessarily involve integro-differential equations, see e.g. Chen et al. [1] for a comparison of different microcontinuum theories and their relation to atomistic models.

is given by

$$\begin{aligned} \rho_0\,\partial_t^2 u(x,t) &= \int_{-\infty}^{+\infty} C(\hat{x}-x)\,[\,u(\hat{x},t)-u(x,t)\,]\;d\hat{x} + b(x,t)\;, \qquad (1.1)\\ (x,t) &\in \mathbb{R}\times(0,T) \end{aligned}$$

where ρ_0 is the constant density, $u(x,t)$ the displacement field for the material point x at time t, C the stiffness distribution density or 'micromodulus' function and b the external force density. If C is a suitable generalized function, (1.1) coincides with the wave equation of local elasticity, see Section 3 for explicit examples. A dispersion analysis of (1.1) gives the angular frequency ω as a function of the wavenumber k:

$$\omega(k) = \left(\int_{-\infty}^{+\infty} [\,1-\cos(k\,\hat{x})\,]\,\frac{C(\hat{x})}{\rho_0}\;d\hat{x}\right)^{1/2}\;. \qquad (1.2)$$

The phase velocity $v_p(k) := \omega(k)/k$ can, in principle, be found experimentally, see e.g. Graff [5]. It can then be used to determine the micromodulus function C according to (1.2). Therefore the nonlocal model (1.1) provides an analytical description of the dynamics of a system characterized by its nonlinear[2] dispersion relation. Weckner & Abeyaratne [6] derived analytical solutions by means of Fourier-transforms which serve as validation problems for the numerical method presented in this paper. For the more general IDE

$$\partial_\tau^2\eta(\zeta,\tau) = \int_{-\infty}^{+\infty} \kappa(\zeta,\xi)\,\eta(\xi,\tau)\;d\xi + \chi(\zeta)\eta(\zeta,\tau) + \varphi(\zeta,\tau) \qquad (1.3)$$

the authors have shown the existence of a unique mild solution η subject to initial conditions $\eta_0(\zeta) := \eta(\zeta,0),\ \nu_0(\zeta) := \partial_\tau\eta(\zeta,0)$ in the function space of Bochner-integrable abstract functions with values in $L^\infty(\mathbb{R})$, the space of essentially bounded functions, see Emmrich & Weckner [7]. The solution η can be interpreted as the normalized displacement of an inhomogeneous bar. In general, all quantities denoted by Greek letters are dimensionless (except ρ_0, ω). In agreement with Weckner & Abeyaratne [6], the jump conditions were derived: the Lagrangian location of a discontinuity is shown to remain stationary, which is important for the numerical method presented.

2. **Discretization**

In order to discretize (1.3), we use the Gauß-Hermite quadrature which is exact for any polynomial $\Phi(\xi) \in P_r(\xi)$ of degree $r \le 2\,n-1$:

$$\int_{-\infty}^{+\infty} e^{-\xi^2}\Phi(\xi)d\xi \approx \sum_{k=1}^{n} \sigma_k^{(n)}\Phi(\xi_k^{(n)})\;. \qquad (2.1)$$

Here, $\xi_k^{(n)}$, $k=1,\ldots,n$, are the roots of the Hermite polynomials

$$H^{(n)}(\xi) := \frac{(-1)^n}{(2^n n!\sqrt{\pi})^{1/2}}\;e^{\xi^2}\,\frac{d^n}{d\xi^n}(e^{-\xi^2})$$

[2]The wave equation of classical elasticity theory corresponds to a linear dispersion relation.

which we arrange such that $\xi_k^{(n)} < \xi_{k+1}^{(n)}$; the weights $\sigma_k^{(n)}$ are defined by $\sigma_k^{(n)} := \int_{-\infty}^{+\infty} e^{-\xi^2} L_k^{(n)}(\xi) d\xi$ with the Lagrange polynomials $L_k^{(n)}(\xi) := \prod_{j=1, j\neq k}^{n} \frac{\xi - \xi_j^{(n)}}{\xi_k^{(n)} - \xi_j^{(n)}}$. We set $\Phi(\xi;\zeta,\tau) = e^{\xi^2}\kappa(\zeta,\xi)\,\eta(\xi,\tau)$ for the approximation of the improper integral in (1.3). The method of collocation then leads to the following set of ordinary differential equations (ODEs)

$$\ddot{\eta}_j^{(n)}(\tau) = \sum_{k=1}^{n} \sigma_k^{(n)} e^{\xi_k^{(n)2}} \kappa(\xi_j^{(n)}, \xi_k^{(n)}) \eta_k^{(n)}(\tau) + \chi(\xi_j^{(n)}) \eta_j^{(n)}(\tau) + \varphi(\xi_j^{(n)}, \tau)\,, \qquad (2.2)$$

where $\eta_j^{(n)}(\tau),\ j = 1,\ldots,n$, are approximations for $\eta(\xi_j^{(n)},\tau)$. Introducing the notation $\underset{\sim}{\eta}(\tau) := (\eta_j^{(n)}(\tau))$, $\underset{\sim}{\Gamma} := (\Gamma_{j,k}) = (-\sigma_k^{(n)} e^{\xi_k^{(n)2}} \kappa(\xi_j^{(n)}, \xi_k^{(n)}) - \chi(\xi_k^{(n)})\,\delta_{j,k})$, $\underset{\sim}{\varphi}(\tau) := (\varphi(\xi_j^{(n)},\tau))$, where $\delta_{j,k}$ is the Kronecker symbol, one can rewrite the discretized equation of motion (2.2) as

$$\ddot{\underset{\sim}{\eta}}(\tau) + \underset{\sim}{\Gamma}\,\underset{\sim}{\eta}(\tau) = \underset{\sim}{\varphi}(\tau)\ . \qquad (2.3)$$

Note that the stiffness-matrix $\underset{\sim}{\Gamma}$ is *not* symmetric. Fourier-transformation leads to $\underset{\sim}{\underset{\sim}{\Pi}}(\mu)\bar{\underset{\sim}{\eta}}(\mu) = \bar{\underset{\sim}{\varphi}}(\mu)$ with the dynamical stiffness-matrix $\underset{\sim}{\underset{\sim}{\Pi}}(\mu) = \underset{\sim}{\Gamma} - \mu^2\,\underset{\sim}{1}$ and the identity matrix $\underset{\sim}{1}$.

The solution of the homogeneous problem, $\underset{\sim}{\Gamma}\,\bar{\underset{\sim}{\eta}}^h(\mu) = \lambda\ \bar{\underset{\sim}{\eta}}^h(\mu)$, is

$$\underset{\sim}{\eta}^h(\tau) = \sum_{j=1}^{n} \left(\alpha_j \hat{\underset{\sim}{\eta}}_j \cos(\mu_j \tau) + \beta_j \hat{\underset{\sim}{\eta}}_j \sin(\mu_j \tau) \right) \qquad (2.4)$$

with the semi-simple eigenvalues of the stiffness matrix $\lambda_j = \mu_j^2$ and the corresponding eigenvectors $\hat{\underset{\sim}{\eta}}_j$. The $2n$ constants (α_j, β_j) are determined by the initial conditions by solving the set of linear equations

$$\underset{\sim}{\eta}(\tau = 0) = (\eta_0(\xi_j^{(n)})) = \sum_{j=1}^{n} \alpha_j \hat{\underset{\sim}{\eta}}_j,\ \dot{\underset{\sim}{\eta}}(\tau = 0) = (\nu_0(\xi_j^{(n)})) = \sum_{j=1}^{n} \beta_j \mu_j \hat{\underset{\sim}{\eta}}_j\ . \qquad (2.5)$$

Therefore, one can solve the discretized equation of motion (2.2) in two ways: either one uses a time step integration scheme (such as Runge-Kutta or Newmark) or one uses an eigenvalue solver to obtain (2.4) and then solves the above set of linear equations (2.5). The advantage of the second strategy is that the semi-analytical solution allows one to calculate the displacement $\underset{\sim}{\eta}(\tau^*)$ for *any* time τ^* without having to calculate the solution for $\tau < \tau^*$ in advance. In both cases, we find an approximation of the displacement *field* $\eta(\zeta,\tau^*)$ at time τ^* for the *discrete*, not equidistant points $\zeta = \xi_j^{(n)}$ which can then be interpolated to obtain an approximation for an *arbitrary* point $\zeta \in [\xi_1^{(n)}, \xi_n^{(n)}]$. One has to pay special attention to the interpolation of the

numerical results near displacement discontinuites. But since the stationary position of all discontinuities is known in advance, this can easily be done.

3. **Examples**

In order to demonstrate the presented numerical method, we calculate two examples for the homogeneous solution of (1.1) that have been already investigated in detail in Weckner & Abeyaratne [6]. This allows us to validate our numerical results and also discuss its limits.

3.1. **Gaussian initial displacement.** We consider the initial conditions $u_0(x) = Ue^{-(x/L)^2}$, $v_0(x) \equiv 0$ and the micromodulus function $C(x) = \frac{4}{\ell^3}\frac{E}{\sqrt{\pi}}\, e^{-(x/\ell)^2}$ with Young's modulus E and a length scale parameter ℓ. For $\ell \to 0$, (1.1) becomes the wave equation of local elasticity theory:

$$\rho_0\ \partial_t^2 u(x,t) = E\ \partial_x^2 u(x,t) + b(x,t)\ . \tag{3.1}$$

Therefore, ℓ can be seen as a degree of nonlocality. With the normalization $\zeta := x/L$, $c_0 := \sqrt{E/\rho_0}$, $\tau := tc_0/L$, $\eta := u(L\zeta, L\tau/c_0)/U$, $\lambda := \ell/L$, the equation of motion (1.1) can be rewritten as (1.3) with $\kappa(\zeta,\xi) := L^3 C(L(\zeta-\xi))/E$, $\chi(\zeta) := -4\lambda^{-2}$, $\varphi \equiv 0$. The solution of this initial value problem is

$$\eta(\zeta,\tau;\lambda) = \frac{1}{\sqrt{\pi}}\int_0^\infty \cos(\alpha\ \zeta)\ e^{-\alpha^2/4}\cos(\tau\ \sqrt{\frac{1-e^{-\alpha^2\lambda^2/4}}{\lambda^2/4}})\ d\alpha\ , \tag{3.2}$$

see Weckner & Abeyaratne [6]. Expanding (3.2) in a Taylor series around $\lambda = 0$, one obtains the well-known d'Alembert-solution:

$$\lim_{\lambda\to 0} u(\zeta,\tau;\lambda) = U\ \frac{e^{-(\zeta-\tau)^2} + e^{-(\zeta+\tau)^2}}{2}\ . \tag{3.3}$$

We choose $n = 49$ for the quadrature method (2.1) and $\lambda = 3/4$ for the normalized

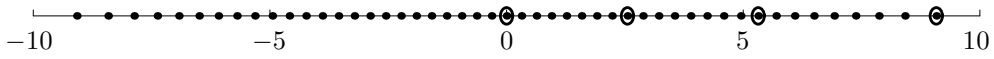

Figure 1. Roots of Hermite polynomials, $n = 49$

length scale parameter. The location of the roots $\xi_k^{(49)}$ of the Hermite polynomials is shown in Figure 1.

The numerical time integration of (2.2) was carried out with the software Mathematica that uses the Livermore Solver LSODE for solving ODEs. The results are compared with the exact solution given by (3.2).[3]

[3]In order to evaluate (3.2), we again use Mathematica. For the following discussion we assume that the (spatial) numerical integration of (3.2) and the (temporal) numerical integration of (2.2) are exact within the resolution of the line thickness. This can be verified by increasing the working precision which does not change the presented numerical and graphical results, respectively.

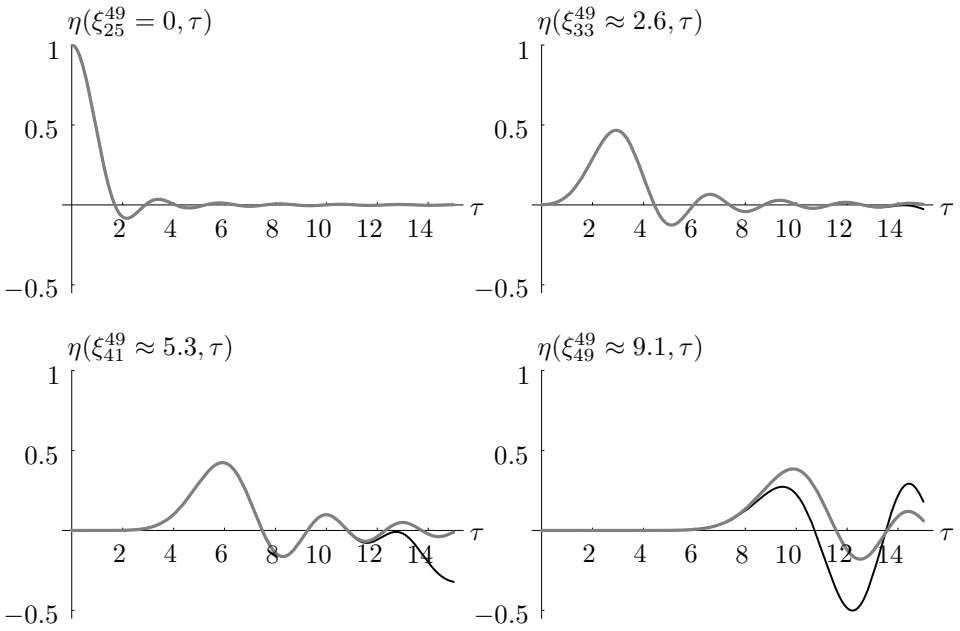

Figure 2. Plots of the displacement $\eta_k(\tau)$ for fixed points: numerical (black line) and analytical results (grey line) of Example 3.1

Figure 2 presents a plot of the displacement $\eta_k^{(n)}(\tau)$ as a function of time for the fixed points $\xi_{25}^{(49)}, \xi_{33}^{(49)}, \xi_{41}^{(49)}, \xi_{49}^{(49)}$ marked by circles in Figure 1. Figure 3 shows the spatially interpolated displacement field $\eta(\zeta, \tau_k)$ for the fixed times $\tau_k = k, k = 0, \ldots, 11$, using piecewise cubic polynomials. Since the system is symmetric with respect to the axis $\zeta = 0$, we only plot the half-plane $\zeta \geq 0$. Both figures show that the numerical results agree well with the analytical results for all the points $\zeta \in [\, \xi_1^{(49)} \approx -9.1, \xi_{49}^{(49)} \approx 9.1\,]$ if we limit the time of observation to $\tau < 6$. The difference between the analytical and the (interpolated) numerical solution is shown in Figure 4 whereas the spatial L^2-norm of the error as a function in time is shown in Figure 5.

Increasing the number of integration points extends both the spatial and temporal observation interval. The valid temporal observation period can also be extended if we restrict our attention to points closer to the origin: the displacement of the particle located *at* the origin $0 = \eta_{25}^{(49)}$ is correct until $\tau \approx 14$.

For $\tau > 14$, the analytical solution and our numerical approximation do not agree any more for *any* particle. This is caused by the reflection of elastic waves at the numerically induced artificial boundary. The type of boundary conditions introduced in this example is dictated by the quadrature method used. In future research, it would be interesting to study the problem of wave reflection in Peridynamics in more detail which to the knowledge of the authors has not been previously pursued. It might

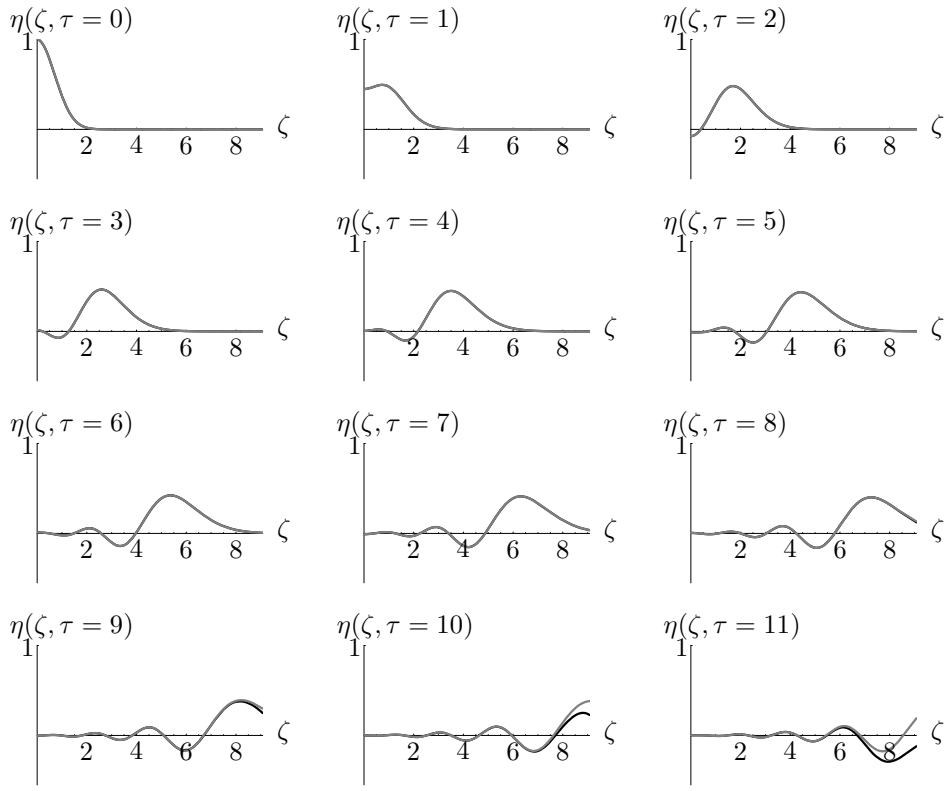

Figure 3. Snapshots of the spatially interpolated displacement field $\eta(\zeta, \tau_k)$ for fixed times $\tau_k = k, k = 0, \ldots, 11$: numerical (black line) and analytical results (grey line) of Example 3.1

be possible to introduce absorbing, non-reflecting boundary conditions to further improve the above results.

3.2. **A Riemann-like problem.** In this example, we look at a bar initially at rest with a piecewise constant velocity field involving a jump at the origin: $v_0(x) = v_- h(-x) + v_+ h(x)$ where $h(\cdot)$ denotes the unit step function. The aim is to investigate how well the presented numerical method copes with discontinuous initial conditions. The material considered is[4] $C(x) = \frac{E}{\pi \ell^3} \frac{2\sin(x/\ell) - 2(x/\ell)\cos(x/\ell)}{(x/\ell)^3}$ corresponding to a continuous piecewise linear dispersion relation (1.2). According to Weckner &

[4]We again choose the stiffness distribution such that for $\ell \to 0$ the equation of motion (1.1) becomes the wave equation (3.1).

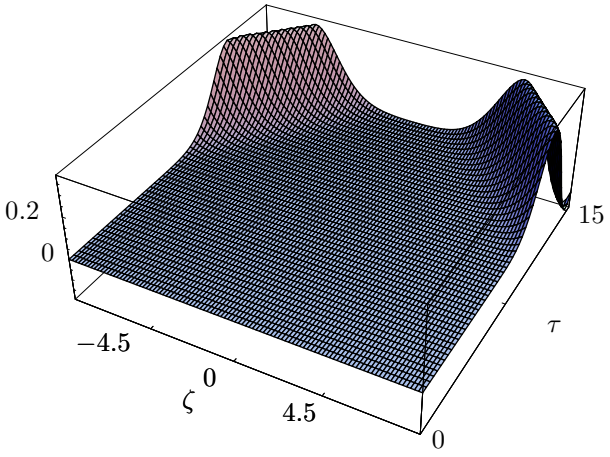

Figure 4. Error between the exact displacement field $\eta(\zeta,\tau)$ and the numerical one for Example 3.1 with $\zeta \in [\xi_1^{49} \approx -9.1, \xi_{49}^{49} \approx 9.1]$ and $\tau < 15$

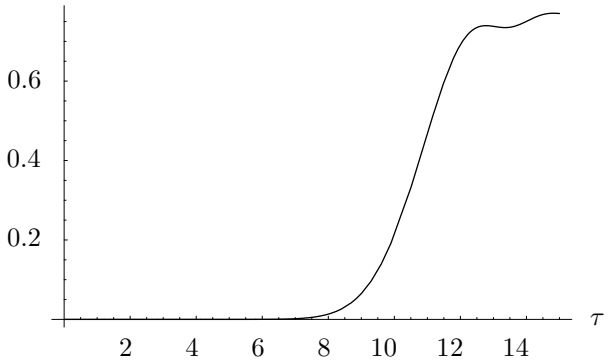

Figure 5. L^2-norm of the error between the exact displacement field $\eta(\zeta,\tau)$ and the numerical one for Example 3.1 for $\tau < 15$

Abeyaratne [6], the resulting displacement field is:

$$\begin{aligned}\eta(\zeta,\tau) \;=\; & \frac{V_+ + V_-}{2}\,\tau \\ & + \frac{V_+ - V_-}{4\pi}\;\big[\,(\zeta+\tau)\;\mathrm{Si}(\zeta+\tau) - (\zeta-\tau)\;\mathrm{Si}(\zeta-\tau) \\ & \qquad + \sin(\tau)\,(\pi\;\mathrm{sgn}(\zeta) - 2\;\sin(\zeta) - 2\;\mathrm{Si}(\zeta))\;\big]\;,\end{aligned} \tag{3.4}$$

with $\zeta := x/\ell$, $c_0 := \sqrt{E/\rho_0}$, $\tau := c_0 t/\ell$, $\eta(\zeta,\tau) := \frac{u(\zeta\ell,\tau\ell/c_0)}{\ell}$, $V_\pm := v_\pm/c_0$. Si$(\cdot)$ is the integral sine function and sgn$(\cdot)$ is the sign function.
For the numerical simulation, we choose $n = 49$, $V_+ = -V_- = 1$. In Figure 6, the analytical solution (3.2) is drawn as a grey line whereas the numerical solution is drawn as a dashed, black line. As in the previous Example 3.1, the numerical results agree well with the analytical results for a finite time and spatial interval.

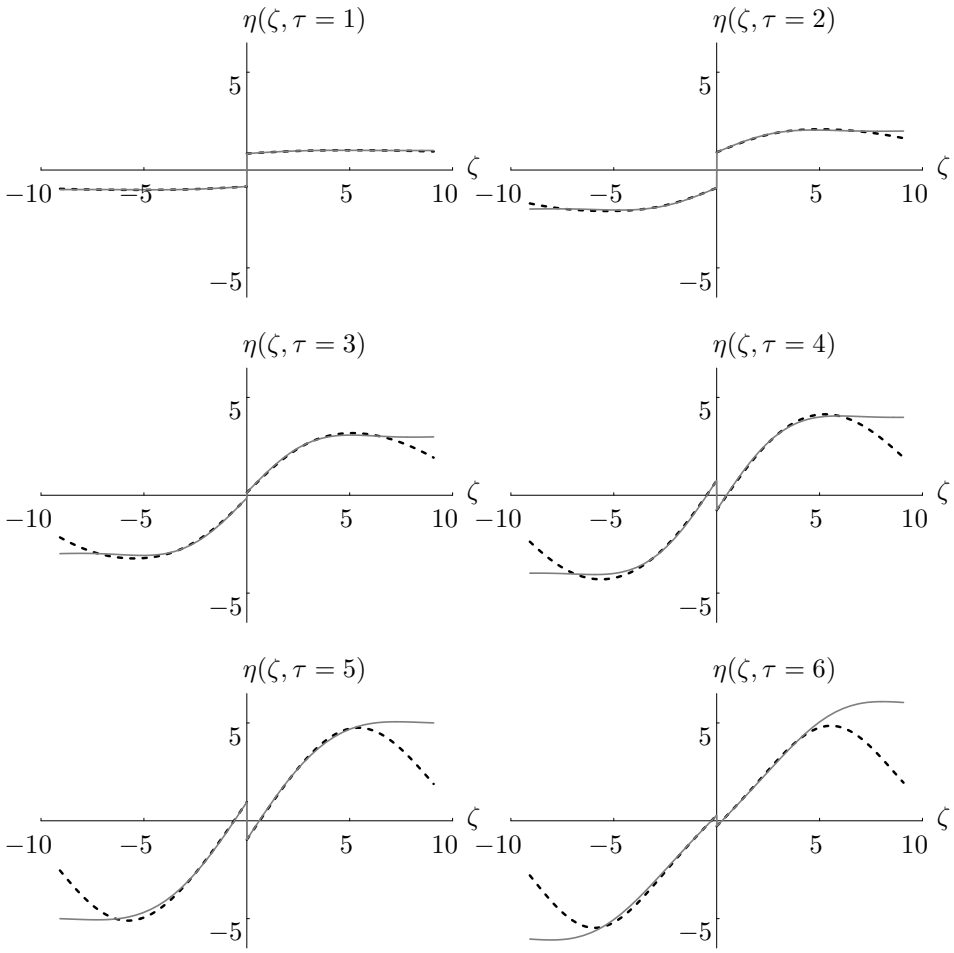

Figure 6. Snapshots of the spatially interpolated displacement field $\eta(\zeta,\tau_k)$ for fixed times $\tau_k = k, k = 0,\ldots,6$: numerical (dashed, black line) and analytical results (grey line) of Example 3.2

4. **Conclusions**

As the two Examples 3.1 and 3.2 show, the numerical method presented can efficiently be used to calculate approximate solutions of the IDE (1.1), even in the case of discontinuous initial data. An agreement with the exact solution, however, can only be expected in a finite spatial domain up to a finite time. This is due to the approximation of the improper integral by a finite sum which can be interpreted as the introduction of artificial boundaries.

Changing the (possibly inhomogeneous) material properties can easily be implemented by redefining the functions $\kappa(\zeta, \xi)$ and $\varphi(\zeta)$ accordingly. Future work will concentrate on extending the presented method to problems in two and three dimensions and to the nonlinear case.

Acknowledgement. This work was supported by a fellowship of the first author within the Postdoc-Programme of the German Academic Exchange Service (DAAD).

REFERENCES

1. Chen, Y., Lee, J., and Eskandarian, A.: Atomistic viewpoint of the applicability of microcontinuum theories. *Int. J. Solids Structures*, **41**, 2004, 2085–2097.
2. Silling, S. A.: Reformulation of elasticity theory for discontinuities and long-range forces. *J. Mech. Phys. Solids*, **48**, 2000, 175–209.
3. Kunin, I. A.: *Elastic Media with Microstructure I.* Springer-Verlag, Berlin, 1982.
4. Rogula, D. (ed.): *Nonlocal Theory of Material Media.* Springer-Verlag, Wien, 1982.
5. Graff, K. F.: *Wave Motion in Elastic Solids.* Dover Publications, New York, 1991.
6. Weckner, O. and Abeyaratne, R.: The effect of long-range forces on the dynamics of a bar. *J. Mech. Phys. Solids* **53**, 2005, 705–728.
7. Emmrich, E. and Weckner, O.: Analysis and numerical approximation of an integro-differential equation modelling non-local effects in linear elasticity. *Math. Mech. Solids*, online, December, 2005, DOI No. 10.1177/1081286505059748.